





Phenotypic Profiling of Macrocyclic Lactones on Parasitic *Schistosoma* Flatworms

Kaetlyn T. Ryan,^a Nicolas J. Wheeler,^{a,b} Isaac K. Kamara,^c Hailey Johnson,^c Judith E. Humphries,^d  Mostafa Zamanian,^a  John D. Chan^{a,c}

^aDepartment of Pathobiological Sciences, University of Wisconsin - Madison, Madison, Wisconsin, USA

^bDepartment of Biology, University of Wisconsin - Eau Claire, Eau Claire, Wisconsin, USA

^cDepartment of Chemistry, University of Wisconsin - Oshkosh, Oshkosh, Wisconsin, USA

^dDepartment of Biology, Lawrence University, Appleton, Wisconsin, USA

ABSTRACT Macrocyclic lactones are front-line therapies for parasitic roundworm infections; however, there are no comprehensive studies on the activity of this drug class against parasitic flatworms. Ivermectin is well known to be inactive against flatworms. However, the structure-activity relationship of macrocyclic lactones may vary across phyla, and it is entirely possible other members of this drug class do in fact show antiparasitic activity on flatworms. For example, there are several reports hinting at the anti-schistosomal activity of doramectin and moxidectin. To explore this class further, we developed an automated imaging assay combined with measurement of lactate levels from worm media. This assay was applied to the screening of 21 macrocyclic lactones (avermectins, milbemycins, and others such as spinosyns) against adult schistosomes. These *in vitro* assays identified several macrocyclic lactones (emamectin, milbemycin oxime, and the moxidectin metabolite 23-ketonemadectin) that caused contractile paralysis and lack of lactate production. Several of these were also active against miracidia, which infect the snail intermediate host. Hits prioritized from these *in vitro* assays were administered to mice harboring patent schistosome infections. However, no reduction in worm burden was observed. Nevertheless, these data show the utility of a multiplexed *in vitro* screening platform to quantitatively assess drug action and exclude inactive compounds from a chemical series before proceeding to *in vivo* studies. While the prototypical macrocyclic lactone ivermectin displays minimal activity against adult *Schistosoma mansoni*, this family of compounds does contain schistocidal compounds which may serve as a starting point for development of new anti-flatworm chemotherapies.

KEYWORDS anthelmintic, ivermectin, macrocyclic lactone, schistosomiasis, drug screening

There is a recognized need for new anthelmintics given the limited treatment options for many parasitic infections and the widespread emergence of veterinary drug resistance (1). This problem is particularly acute for the neglected tropical disease schistosomiasis. The current frontline schistosomiasis monotherapy, praziquantel, has been in use for 4 decades. While praziquantel is typically between 70% and 90% effective (2), there are instances of treatment failure (3, 4). Parasite resistance has been selected in laboratory settings, and this is conceivably a risk in the field with more widespread administration of praziquantel monotherapy (5, 6). One barrier that contributes to the scarcity of leads in the development pipeline is that *in vitro* phenotypic screens on adult parasitic worms are often low throughput. The search for new anti-schistosomal compounds has often used schistosomula, the life cycle stage that precedes adult worms (7). However, schistosomula have fewer cells and fewer cell types than adults (8–10), and they have differing sensitivity to some drugs (11). Adult parasites are the disease-causing life cycle stage dwelling within the host, and scalable,

Copyright © 2023 American Society for Microbiology. All Rights Reserved.

Address correspondence to John D. Chan, chanj@uwosh.edu.

The authors declare no conflict of interest.

Received 9 September 2022

Returned for modification 7 October 2022

Accepted 2 January 2023

Published 25 January 2023

quantitative methodologies for screening small molecules against these worms are needed to advance anti-schistosomal drug development.

In this study, we applied automated assays measuring the activity of a specific chemical series, macrocyclic lactones (ML), on adult schistosomes. MLs have a broad spectrum of activity, targeting ligand-gated ion channels (LGICs) of parasites across several phyla (roundworms and arthropods, reviewed in reference 12), as well as numerous vertebrate LGICs (13–16). However, little is known about the structure–activity relationship of MLs in flatworms.

The most commonly used anthelmintic ML, ivermectin, is inactive against intramammalian parasitic flatworms (17–20). Ivermectin is not an agonist on schistosome GluCl isoforms (21). However, ivermectin B_{1b} does kill aquatic life cycle stages of schistosomes (22), and ivermectin does phenocopy praziquantel in several assays on free-living flatworms (23–25). Therefore, despite the lack of activity of ivermectin against intramammalian stages of parasites, this class of compounds is not inactive. Because the structure–activity relationships of MLs can vary depending on the parasite being studied (26), it is possible that other MLs do exhibit potent effects on schistosomes even if ivermectin is relatively inactive. For example, data from human clinical trials (27), screens against schistosomula (28), and computational predictions of anti-schistosomal drugs (29) have indicated moxidectin may have anti-schistosomal effects. These data indicate that at least some MLs do exhibit activity against flatworms, even if they do not act through the GluCl channels that MLs typically target. Therefore, we sought to comprehensively assess the structure–activity relationship of MLs on adult schistosomes using a panel of several phenotypic assays.

RESULTS

***In vitro* measurement of drug activity on adult schistosomes.** *In vitro* phenotypic screening of worms can be challenging because there is not a single outcome that is a reliable predictor of impaired viability within the host *in vivo*. Worm movement is often used as an initial screening outcome, reasoning that dead worms will not exhibit movement. Past methods of quantitatively analyzing adult schistosome movement were manual and low throughput (30), but methods using optical flow algorithms have been developed for automated screening of parasite movement (31–33). These approaches allow for quantitative readouts not biased by subjective scoring; however, on their own do not necessarily provide a readout of worm viability because paralyzed worms may still be alive and recover after drug treatment. Assays benefit from a secondary readout of drug activity, such as lactate measurements from conditioned media which provides a readout of metabolic activity (6, 34). Therefore, we sought to combine these approaches in a multiplexed assay for parasite viability (Fig. 1A). We first optimized assay conditions using two drugs known to paralyze worms *in vitro*, meclonazepam and dichlorvos, and then proceeded to screen 21 commercially available MLs.

Adult parasites were harvested from the mesenteric vasculature of mice 6 to 7 weeks postinfection and allowed to unpair at room temperature. Sexually mature schistosomes live as pairs with the female worm residing within the male ventral gynecophoral canal, although worms tend to unpair during *in vitro* culture. To obtain separate male and female populations for subsequent assays, unpaired female worms were removed from the petri dish and cultured separately. The rationale for using unpaired worms is that if a male and female worm were to unpair in a well, the movement values may be roughly double that of wells with a single male worm. Additionally, female worms lay many eggs (up to ~100 per day) which will accumulate in the well. These eggs will move as worms thrash in the media, producing high motility values because the flow algorithms will detect any pixel that is moving, regardless of whether it is worm or debris. Female worms also contain more ingested food than males. These gut contents are heavily pigmented, containing hemozoin produced from heme in red blood cells. During culture and drug treatment, female worms tend to expel these contents into the well, further confounding the interpretation of flow data.

After harvesting, worms were treated with meclonazepam (10 μ M), which is known to produce contractile paralysis (35), and the cholinergic compound dichlorvos (10 μ M), an acetylcholinesterase inhibitor known to produce flaccid paralysis (36, 37). From visual observation,

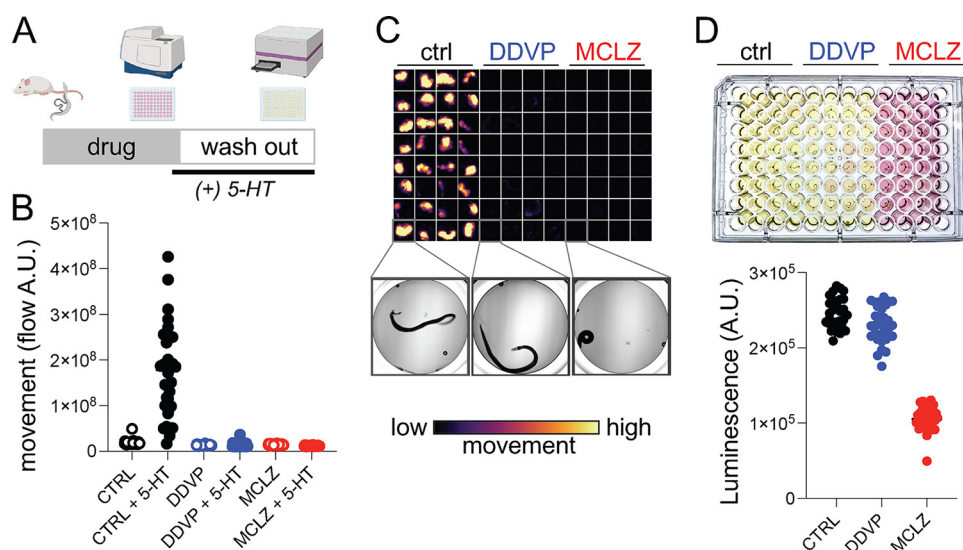


FIG 1 Multiplexed assay for schistosome viability. (A) Drug screening workflow on adult *S. mansoni*. Worms are harvested from mice, exposed to test compounds for 24 h (3 columns or 32 worms/drug), supplemented with 5-HT and imaged to record movement (15 sec/well). Media was changed to fresh drug-free media for follow-up assay measuring lactate production. (B) Quantification of movement for worms exposed to either DMSO control, dichlorvos (DDVP, 10 μ M), or meclonazepam (MCLZ, 10 μ M). Worms were imaged before (open symbols) or after (closed symbols) serotonin addition (5-HT, 250 μ M). (C) Flow cloud showing worm movement over the period of recording for the plate. Yellow areas indicate worm movement, while dark wells remain paralyzed. Below = brightfield images of an individual worm representative of each treatment. (D) Top = plate media after culture (24 h in 5-HT, 250 μ M) to allow accumulation of lactate. Bottom = measurement of lactate from the same plate using the Lactate-Glo assay system.

it was clear that untreated control worms were motile, but the movement was too slow to record within a recording window that allowed for convenient scaling across multiple wells in a plate. Within the recording period of 15 s per well, only a roughly 20% difference in control and drug-treated worms was detectable. Therefore, to expand the signal window between DMSO control and drug treated worms, we supplemented the wells with serotonin (5-HT, 250 μ M) for 1 h prior to recording worm movement (Fig. 1B). This concentration was chosen because it causes maximal stimulation of adult worm movement (38). Adding exogenous 5-HT to the assay does create the opportunity for drug-drug interactions, and this would need to be considered when interpreting the results of compounds that interact with serotonergic signaling pathways (known GPCR ligands, for example). Treatment with 5-HT increased the baseline motility of worms >8-fold relative to control worms without 5-HT. Under these conditions, dichlorvos and meclonazepam inhibited movement by 92% and 93%, respectively, relative to 5-HT treated controls (Fig. 1B and C).

Following motility recordings (Fig. 1B), drug-containing media was removed and replaced with fresh 5-HT containing media (200 μ L per well). Adult schistosomes consume large quantities of glucose (roughly 5 \times their dry body weight each day), and even in the presence of oxygen up to 90% of this glucose is converted into lactic acid (39). The addition of 5-HT, which was required for increasing the signal to noise in the motility assays, also has the benefit of increasing the amount of lactate produced by hyperactive worms (40). Therefore, lactate is a reasonable proxy for adult schistosome metabolic activity, and lactate measurement has been used as schistosome viability assay (6, 34). Lactate levels were quantified using the Lactate-Glo luminescence assay (Fig. 1D). Worms treated with meclonazepam appeared killed by drug treatment, and lactate measurements were 58% less than that of control wells. Dichlorvos treated worms appear to be merely paralyzed but not killed, because these worms produced lactate at levels comparable to control worms (only a 7% decrease) (Fig. 1D). The differences between these two compounds, which both inhibit worm movement, illustrate the utility of using a workflow with multiple readouts to assess drug activity.

In vitro screen of macrocyclic lactones. Using this multiplexed, quantitative assay of worm movement and metabolic activity, we proceeded to profile the activity of commercially available MLs against *Schistosoma mansoni*. These compounds included various avermectins

(which contain a carbohydrate attached to the macrocyclic lactone ring system) and milbemylicins (which lack the carbohydrate), as well as several other members of the class that are more structurally divergent (Fig. 2A; Table S1). Adult parasites were incubated in various concentrations of compound (1 to 20 μM) for 24 h. While most worms did not exhibit changes in morphology with ML treatment, several treatments caused a coiled, contractile phenotype (emamectin, doramectin, milbemylicin oxime, milbemylicin D, 23-ketonemadectin, spinosad; Fig. 2B; Fig. S1). Worms were then imaged in 96-well plates in media supplemented with 5-HT (250 μM), using the motility assay described above. Concentration-response data are summarized in Fig. 2A, with IC_{50} values denoting the concentration at which worm motility was by 50% relative to untreated controls. Compounds that caused obvious changes to worm morphology generally also were effective at inhibiting worm movement relative to controls. However, several compounds that did not cause clear contractile phenotypes were also nonetheless effective at inhibiting movement. For example, eprinomectin-treated worms appeared morphologically normal but their movement was inhibited at drug concentrations 5 μM and above. Full concentration-response curves for all compounds tested are shown in Fig. S2.

Following imaging of worm movement, drug-containing media was replaced with fresh, drug-free culture media supplemented with 5-HT (250 μM). Plates were incubated for a further 24 h to 48 h, and then media was harvested to measure lactate production (Fig. 2A and C). Lactate concentration-response curves were right-shifted relative to the motility readout, indicating that worms are capable of a degree of recovery after drug-washout. Treatments that caused contractile paralysis typically also inhibited lactate production at concentrations that corresponded to maximal movement inhibition. For example, 23-ketonemadectin caused complete contractile paralysis of worms at 10 μM and also completely inhibited movement and lactate production at this concentration. However, at lower concentrations, movement was partially inhibited while lactate remained relatively unchanged. Finally, not all treatments that caused contractile paralysis killed worms. For example, spinosad and doramectin treated worms displayed clear changes in morphology (Fig. 2B) and movement was inhibited (Fig. 2C); however, following drug washout, these worms recovered and produced lactate at levels comparable to controls at all concentrations tested.

In other organisms, MLs act through activation of inhibitory LGICs (41). Another compound that works through activation of inhibitory LGICs and has activity on *S. mansoni* is the benzodiazepine meclonazepam (42). However, meclonazepam does not exhibit activity against all species of schistosomes; *Schistosoma japonicum* are unaffected by this compound (35). Therefore, we were interested in whether MLs may also be inactive against this species. Adult *S. japonicum* were harvested from mice 7 weeks postinfection and treated with a selection of compounds that displayed activity on *S. mansoni* (23-ketonemadectin, emamectin, milbemylicin oxime, and doramectin). All hits that were active against *S. mansoni* also displayed activity against *S. japonicum*, causing contractile paralysis (Fig. 3A) and inhibition of motility and lactate production (Fig. 3B). These data indicate that MLs may be capable of targeting multiple species of parasites.

The activity of MLs on adult schistosomes is of clear interest because this life cycle stage dwells within infected humans. However, one of the few published reports of ML activity on schistosomes is on the life cycle stage that emerges from the snail intermediate host (22). To determine whether the activity profile we observed in adults may also hold for other life cycle stages, we performed a motility assay on *S. mansoni* miracidia hatched from eggs isolated from the livers of *S. mansoni*-infected mice. Miracidia were aliquoted into 24-well plates and incubated in drug-containing artificial pond water. A selection of MLs were screened at a fixed concentration of 5 μM . This concentration was chosen because it represents an intermediate concentration at which more potent compounds displayed activity against adult worms while less active compounds showed no discernible effect. Videos of worm motility (30 s each) were recorded after a 1-h drug incubation period. Praziquantel (3 μM) was chosen as a positive control because this concentration was previously reported to kill miracidia (43). The image stacks from the acquired videos were processed to provide a single minimum intensity projection for each well, providing a proxy for worm movement over the recording

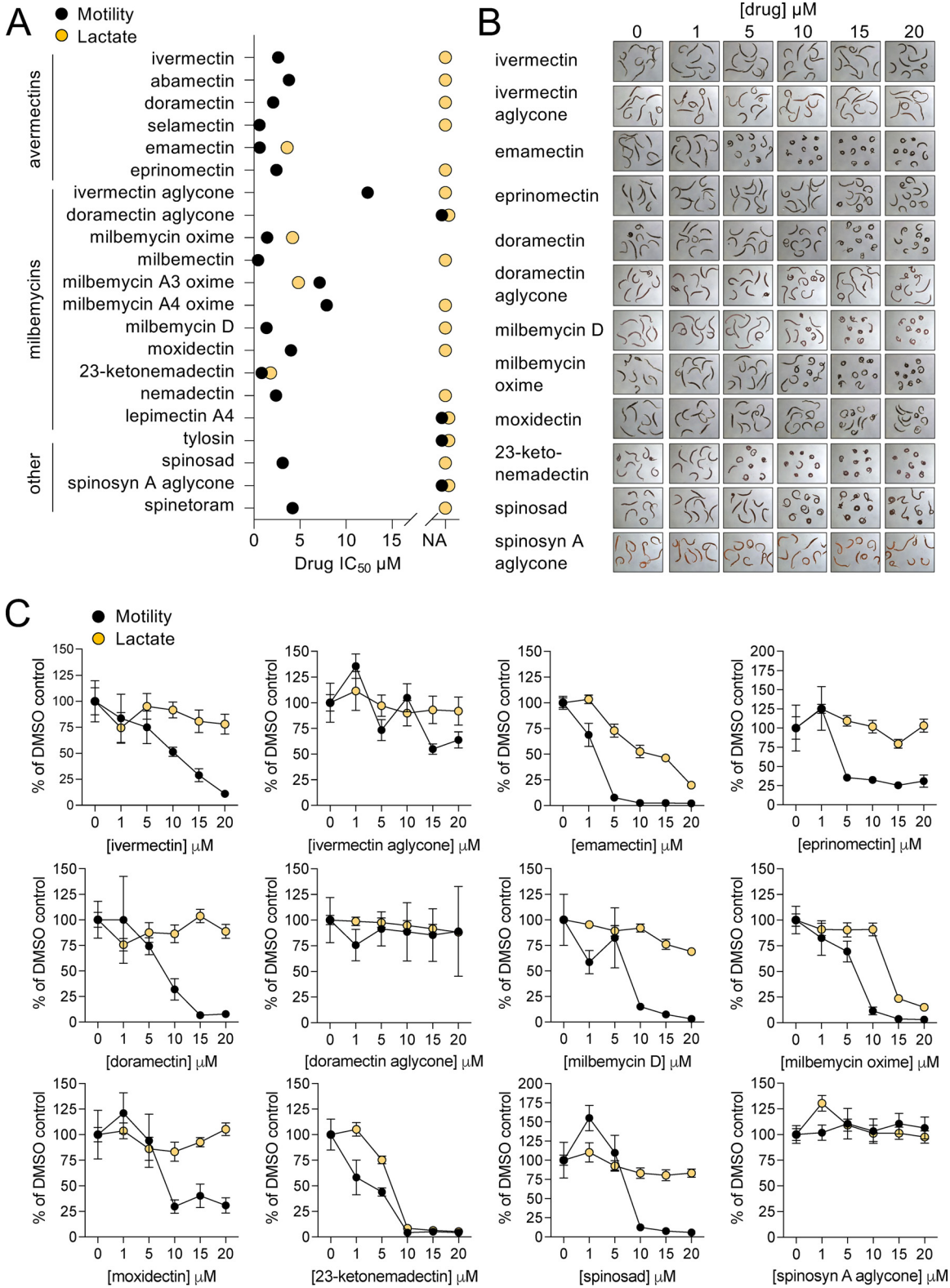


FIG 2 *In vitro* effect of macrocyclic lactones on adult *S. mansoni*. (A) Summary of IC₅₀ values from motility and lactate assay concentration-response screens on 21 macrocyclic lactones. NA = no inhibition relative to controls, no IC₅₀ value could be determined. Adult male *S. mansoni* were cultured in drug for 24 h (1 column or 8 worms per drug concentration) and then assayed for movement and lactate production as per Fig. 1. Motility is shown in black symbols and lactate assays in orange. (B) Images of adult male worms treated with various concentrations of drug, showing concentration-dependent effects on worm morphology for certain compounds. (C) Concentration-response curves for compounds shown in B, plotted with motility (black) and lactate (orange) reflecting mean ± standard error. Concentration-response curves for all 21 compounds listed in (A) can be found in Fig. S2.

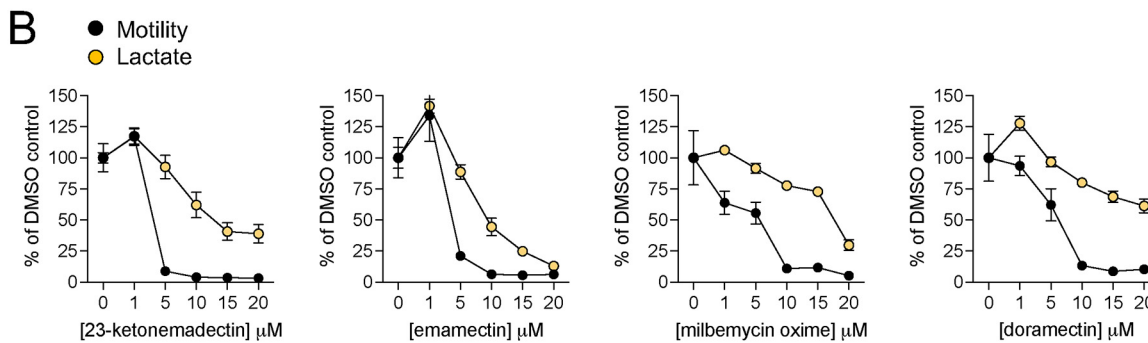
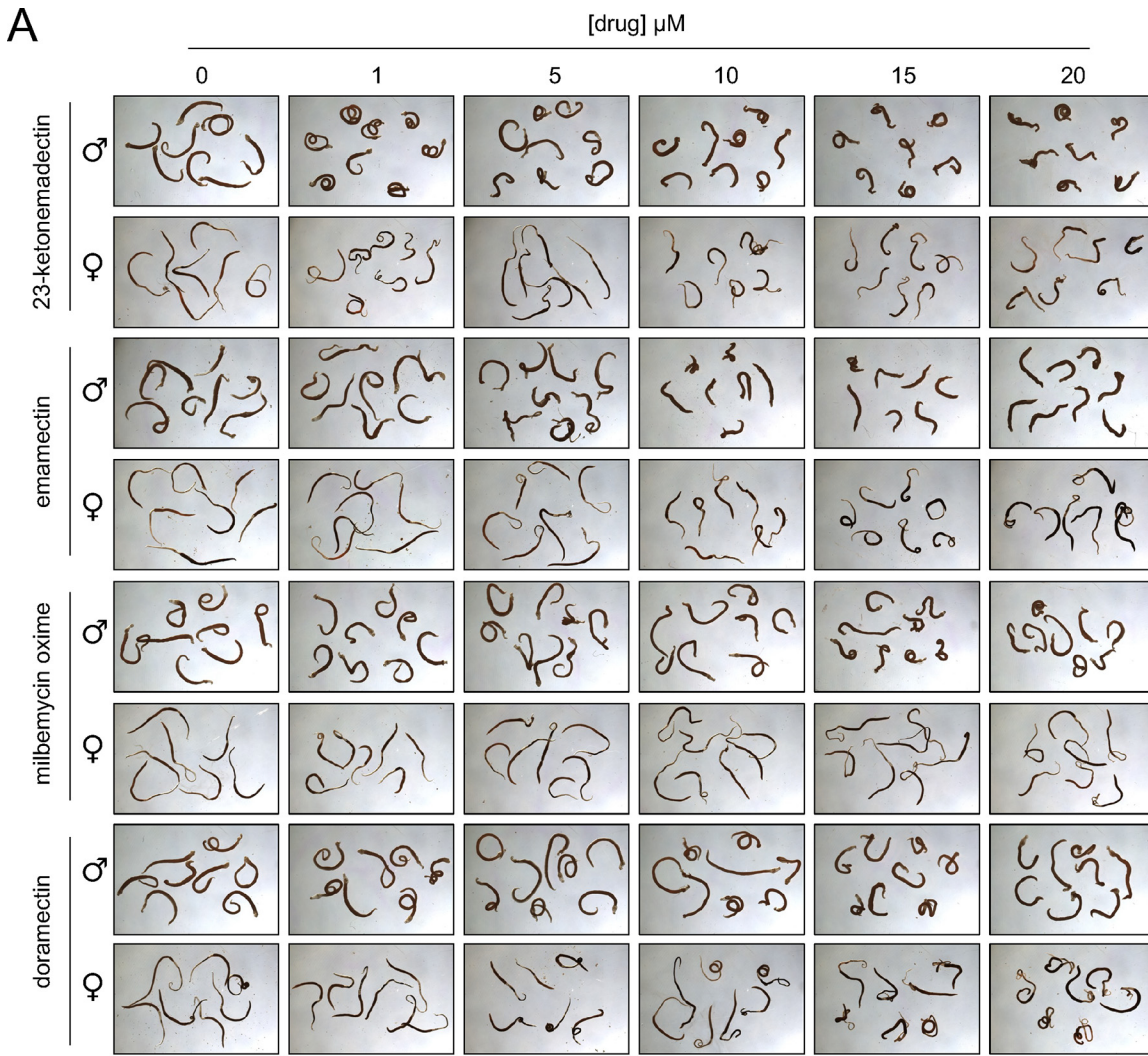


FIG 3 Activity of macrocyclic lactones on adult *S. japonicum*. (A) Morphology of adult male and female worms treated with selected macrocyclic lactones active on *S. mansoni* (23-ketonemadectin, emamectin, milbemycin oxime, doramectin). (B) Concentration = response curves for motility (black) and lactate production (orange) of worms treated with drugs shown in (A). Symbols reflect mean \pm standard error.

period. Paths of individual miracidia can be inferred from dark trails across the images (Fig. 4). This provides a qualitative readout of whether worms in the wells exhibit movement or not. Because miracidia also swim rapidly up and down in the Z axis, entering and leaving the focal plane, quantitative analysis of individual worm movement from these videos is more difficult. However, these minimum intensity projections allow for simple scoring of whether miracidial movement does or does not occur for a given treatment. The results were consistent across replicates that milbemycin oxime and 23-ketonemadectin were active against miracidia (0/6

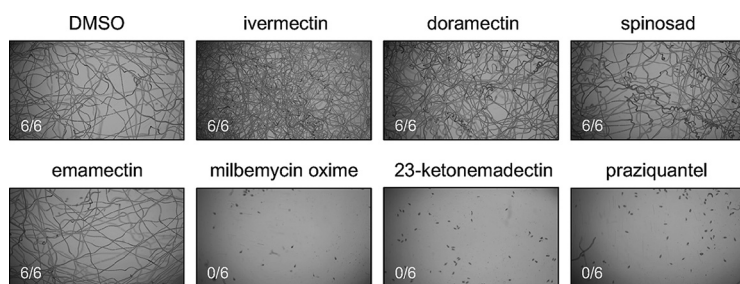


FIG 4 Activity of macrocyclic lactones against *S. mansoni* miracidia. Freshly hatched *S. mansoni* miracidia were incubated in either DMSO, test compound (5 μ M each ML), or praziquantel (3 μ M) for 1 h. Movement was recorded for 30 s, and the resulting image stacks were processed to produce the maximum intensity projections shown above. Each drug treatment was repeated as 6 technical replicates, the scored number shown reflects wells with worm movement.

replicates moving for each). Ivermectin and doramectin, which were less effective against adult worms, did not obviously reduce movement relative to DMSO controls.

In vivo activity of macrocyclic lactones against *S. mansoni*. We proceeded to test the *in vivo* efficacy of several MLs in a murine model of schistosomiasis. Prior studies on the ML doramectin reported that this drug reduced *S. mansoni* parasite burden in mice by 60% (28). In addition to doramectin (30 mg/kg), we chose to test emamectin (20 mg/kg), 23-ketonemadectin (12.5 mg/kg) and milbemycin oxime (100 mg/kg) because of the activity of these compounds in motility and lactate assays. Ivermectin (10 mg/kg) was selected as a negative control as it has been extensively reported as inactive against schistosomes, and eprinomectin (20 mg/kg) was also selected due to the structural similarity to emamectin. Meclonazepam (30 mg/kg) was selected as a positive control given its established efficacy against *S. mansoni* in rodents (35) and humans (44). Female Swiss Webster mice harboring 6-week *S. mansoni* infections were administered compounds by oral gavage. Doses were chosen to be as close to the maximum tolerated dose as possible while not exhibiting toxic effects. These doses are much higher than those typically given to treat parasitic nematodes. For example, ivermectin is typically dosed in the range of 100 to 200 μ g/kg (45). Rodent oral LD₅₀ toxicity data were used to inform the doses chosen in this study (45, 46), or literature on previous studies on murine models (28, 47). Animals were sacrificed 1 week later to count parasite burden. No reduction in worm burden was observed for any treatment (Fig. 5), despite the relatively high doses of compound administered.

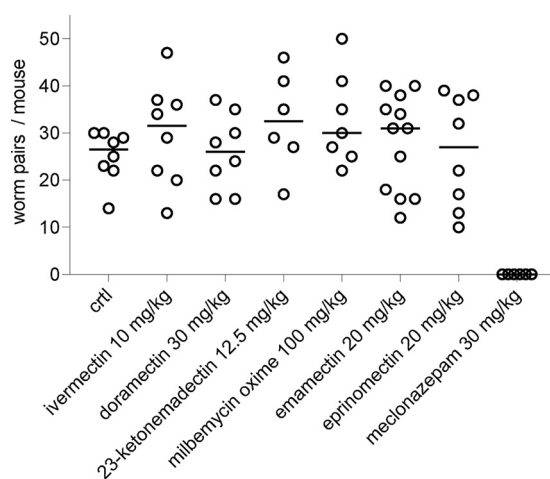


FIG 5 *In vivo* efficacy of macrocyclic lactones against adult *S. mansoni*. Mice harboring patent schistosome infections were treated orally with either vehicle negative control, various MLs, or meclonazepam (positive control) at the dose indicated. Open symbol = worm burden of an individual mouse, solid bar = mean worm burden.

DISCUSSION

MLs are considered ineffective against parasitic flatworm infection, largely due to studies that have shown ivermectin to be inactive on these worms (17–19). However, there are scattered reports of other MLs that do exhibit activity on flatworms *in vitro* or *in vivo* (22, 23, 27, 28). To explore this chemical series further, we screened 21 MLs (avermectins, milbemycins, spinosyns) and identified several MLs active *in vitro* against *S. mansoni* and *S. japonicum*.

Quantitative multiplexed assay for movement and metabolic activity. We looked at several different endpoints to assess ML activity, and the profile of different compounds varied across these assays. Motility assays tended to be more sensitive, 16/21 compounds inhibited movement to some degree at the concentrations tested (Fig. 2A). These include many treatments which did not exhibit obvious changes in worm morphology such as curling/contraction. However, inhibited movement does not necessarily indicate a particularly deleterious effect of drug on the parasite. Following drug washout, many worms seem quite capable of recovering. This is indicated by the right shift in potency of the concentration—response curves in the lactate measurement assay relative to the motility assays (Fig. 2; Fig. S2). In fact, some treatments that caused near complete inhibition of movement had no effect on lactate production after washout (i.e., eprinomectin, doramectin, spinosad). A few compounds did show activity in all endpoints—emamectin, milbemycin oxime and 23-ketonemadectin caused contractile paralysis and inhibition of movement and lactate production. Several MLs have been screened against schistosomes as part of a larger library (28); however, the activity of these three compounds has not been previously reported.

These data provide an example of the utility of obtaining multiple readouts from an *in vitro* drug screen. Integrating additional endpoints is possible given the power of high content imaging systems and the range of assays developed on different worms (7, 33, 48–52). For example, additional steps could conceivably be incorporated to image tegument damage—an important parasite response to some antischistosomal compounds such as praziquantel. These assays could be developed using fluorescent-conjugated antibodies against known tegument antigens. The decision to increase the number of endpoints may depend on the intent of the screen, as there is some trade-off between increased workflow complexity (i.e., blocking, staining, and washing steps involved with immunocytochemistry) and assay throughput.

Notably, all of the compounds we tested were inactive *in vivo* (Fig. 5). This included doramectin, which had subcurative efficacy in another murine model (28). However, the Liberian strain of *S. mansoni* and NMRI line of mice used in that study differ from the parasite and host strains provided by the NIH-NIAID Schistosomiasis Resource Center (NMRI *S. mansoni* in Swiss Webster mice). Variability in drug screening results between laboratories that use different parasite and mouse strains has been reported (28, 53). Our *in vitro* data (Fig. 2 and 3) show that compounds exhibit activity in the low micromolar range when incubated for 24 h. While adult *S. mansoni* reside in the mesenteric vasculature and would be transiently exposed to higher concentrations of drug prior to first pass-metabolism, it is likely that the free-drug concentration that worms are exposed to *in vivo* is below micromolar concentrations over a period of 24 h, particularly in a murine model where mice have more rapid metabolism than humans. This issue of whether *in vitro* concentrations of drug can be therapeutically achieved *in vivo* has also been raised regarding the repurposing of ivermectin as a SARS-CoV-2 therapy. Ivermectin exhibited antiviral effects *in vitro* at 5 μ M, but *in vivo* only reaches submicromolar plasma concentrations—and even then much of the drug is protein bound (54). Nevertheless, our data still show that MLs as a class can exhibit schistocidal activity. In this study, we only screened 21 compounds against schistosomes, while hundreds of MLs have been screened to yield the nematicidal compounds currently in use (26). Further exploration of this chemical series is likely to produce more potent hits.

Structure-activity relationship of MLs on *S. mansoni*. Consistent with prior studies, ivermectin did not exhibit schistocidal activity. However, other members of the class were capable of killing worms *in vitro* (Fig. 2). These were not restricted to one group of compounds (i.e., just avermectins or just milbemycins), or molecules with specific functional groups. Generally, the structure-activity relationship reproduced several observations reported for

MLs on other organisms. Some observations can be made regarding substituents on the carbohydrate, benzofuran, and spiroketal rings.

Several aglycones, which are missing the carbohydrate ring system, were tested and all were inactive (Fig. 2C). This is consistent with data from nematodes showing that the aglycones, which contain a polar hydroxy group on the C-13 position, are inactive while the milbemycins, which also lack the sugar molecule at this position, retain activity (26). Comparison of emamectin, eprinomectin, and abamectin is also useful for determining the importance of substitution at the carbohydrate C4 position. Emamectin was more capable of killing worms than eprinomectin. Emamectin contains a methylamino group at the carbohydrate C4 position, while eprinomectin contains an acetylamino group. This is in contrast to abamectin, which contains a hydroxy group at this position and exhibits even less activity (Fig. 2A; Fig. S2).

The activity of milbemycin oxime, and to a lesser extent selamectin, indicates schistosomes may be amenable to substitution of the C5 position of the benzofuran ring with an oxime. These compounds displayed comparable activity to others with a C5 hydroxy group. This is in contrast to nematodes, which are less tolerant of C5 substitutions (26, 55).

Modification of the spiroketal ring system also alters drug activity. Differences in schistocidal and molluscicidal activity have been reported for ivermectin; ivermectin B1_a contains a sec-butyl group and is relatively inactive (unlike what is observed in nematodes) while ivermectin B1_b contains a isopropyl group on the spiroketal ring and is more active (22). A particularly interesting pair of compounds from this study are moxidectin and its metabolite 23-ketonemadectin. Moxidectin did not cause contractile paralysis of worms. While it did partially inhibit movement, it had no impact on lactate production. Treatment with 23-ketonemadectin, which differs from moxidectin in that it possesses a ketone group rather than a methoxyamine at the C23 position of the spiroketal ring, caused contractile paralysis, inhibition of movement, and lack of lactate production. Given the schistocidal activity of 23-ketonemadectin *in vitro*, it is possible that this metabolite contributes to the 70% *S. mansoni* egg reduction rate observed in humans treated with moxidectin (27).

ML mechanism of action on flatworms. These *in vitro* data raise the question of what is the target and mechanism of action for MLs in flatworms that underpins paralysis and death? In free-living *Caenorhabditis elegans*, MLs target inhibitory LGICs while also requiring connections between adjacent cells/tissues to propagate the nematicidal effects (56). In parasitic nematodes, the therapeutic mechanism of MLs may involve inhibiting the release of excretory-secretory vesicles and proteins (57–60). Even if LGICs are relatively conserved across roundworms and flatworms and MLs are also acting on inhibitory schistosome LGICs, flatworm and nematode anatomy is quite different and, therefore, the drug mechanisms are likely to differ between the two phyla.

MLs certainly have a wide range of targets—some are LGICs and some are not (61, 62). The flatworm target of these compounds is likely not a GluCl. The GluCl ivermectin binding requires a glycine residue at a specific transmembrane domain (63). Schistosomes contain phenylalanine or isoleucine at this position—both of which contain much larger side chains that make this pocket inaccessible to drugs (64). This has been confirmed by cloning and heterologous expression of *S. mansoni* GluCl, which have been shown to be insensitive to ivermectin (21). However, consideration of potential targets does not need to be restricted to GluCl because MLs are relatively promiscuous ligands that have been shown to act on numerous different types of LGICs (13, 14, 16, 65, 66).

In addition to GluCl, schistosomes possess acetylcholine-gated chloride channels (ACCs) (67), nicotinic acetylcholine receptors (nAChRs) which are predicted to be cationic (68), and a clade of unique channels which lack the Cys-loop motif that typically defines LGICs (69). If MLs were to be acting on a schistosome LGIC, cationic nAChRs are potential targets to be explored. In insects, a nAChR is the target of the spinosyns (70–74), which in schistosomes cause the same contractile phenotype as the avermectins and milbemycins (Fig. 2B). This phenotype is more consistent with cation influx than the action of inhibitory channels, which may be expected to cause flaccid paralysis. Studies on recombinantly expressed human $\alpha 7$ nAChRs and $\alpha 4\beta 2$ nAChRs found them to be sensitive to emamectin, but not ivermectin (75), which would be consistent with emamectin having greater activity

on schistosomes (Fig. 2). A separate ML binding site within nAChRs has been proposed: an “intrasubunit” site, that is distinct from the intersubunit site that is blocked by large schistosome amino acid side chains (64). The potency of avermectin-type MLs on nAChRs is also lower, in the micromolar range, which is more in line with the concentrations of drug used in this study than what is observed on GluCl_s. These data point to nAChRs as potential interesting targets to explore, although functional expression of parasite nAChRs is not trivial as this can involve iterating through heteromeric subunit combinations and may require various accessory subunits (76).

MATERIALS AND METHODS

Harvesting adult schistosomes. Female Swiss Webster mice infected with either *S. mansoni* (NMRI strain) or *S. japonicum* (Philippine strain) were sourced from the NIH-NIAID Schistosomiasis Resource Center. Mice were euthanized by CO₂ asphyxiation between 6 and 7 weeks postinfection and adult schistosomes were harvested from the mesenteric vasculature. Livers were set aside in ice-cold 1.2% NaCl and saved for miracidia hatching as mentioned below. Adult worms were placed in culture media consisting of high-glucose DMEM supplemented with 5% fetal calf serum, penicillin-streptomycin (100 units/mL), HEPES (25 mM) and sodium pyruvate (1 mM). All animal work, including *in vivo* drug treatments outlined below, were carried out with the oversight and approval of UW-Madison Research Animal Resources and Compliance (RARC), adhering to the humane standards for the health and welfare of animals used for biomedical purposes defined by the Animal Welfare Act and the Health Research Extension Act. Experiments were approved by the UW-Madison School of Veterinary Medicine IACUC committee (approved protocol #V006353-A08).

Sourcing test compounds. Compounds were sourced as follows: dichlorvos (MilliporeSigma), meclonazepam (Toronto Research Chemicals), ivermectin (Alfa Aesar), abamectin (Thermo Fisher Scientific), doramectin (Selleck Chemicals, Thermo Fisher Scientific), selamectin (Cayman Chemical, MedChemExpress), emamectin (Santa Cruz Biotechnology), eprinomectin (MilliporeSigma), ivermectin aglycone (Cayman Chemical), doramectin aglycone (Cayman Chemical), milbemycin oxime (MedChemExpress, TargetMol), milbemectin (Cayman Chemical), milbemycin A3 oxime (Cayman Chemical), milbemycin A4 oxime (Cayman Chemical), milbemycin D (Toronto Research Chemicals), moxidectin (TCI America), 23-ketonemadectin (Toronto Research Chemicals, United States Biological), nemadectin (Cayman Chemical), lepimectin A4 (Cayman Chemical), tylosin (Ambeed), spinosad (Cayman Chemical), spinosyn A aglycone (Cayman Chemical), spinetoram (Cayman Chemical). Compounds were stored as powder at –20°C and prior to use in experiments were dissolved in DMSO (10 mM). Structures for compounds screened are provided in Table S1.

Adult schistosome motility assays. Worms were harvested from mice, treated with either DMSO control or test compounds listed above, and cultured at 37°C/5% CO₂ for 24 h prior to conducting motility assays. Worms were then imaged in clear 96-well plates on an ImageXpress Nano (Molecular Devices).

Except for experiments shown in Fig. 1B that state otherwise, serotonin (5-HT) was added at 250 μM to increase worm movement at least 1 h prior to imaging. Time lapse recordings were acquired for each well (15 s videos at a rate of 4 frames/second) using a 2× objective. Movement was analyzed using wrmXpress as outlined in [reference 33]. On occasion, individual wells can produce unusually high flow values due to debris or eggs (if paired worms have been inadvertently selected) that are moving in recording as well. Because worm movement should already be close to maximal with addition of 5-HT, high flow readings >3 standard deviations over the mean flow values for a given drug treatment were removed. IC₅₀ values for motility and lactate assays were obtained using the inhibitor versus normalized response function in GraphPad Prism 9.

Lactate assays. Following imaging on the ImageXpress Nano, media was then removed from each well using a multichannel pipette and replaced with fresh culture media supplemented with 5-HT (250 μM). Depending on the volume of media placed in the well, the time for lactate accumulation will vary as lactate is more dilute in larger media volumes. The assay was performed at 1 day incubation per 200 μL of media (i.e., either 1 day incubation in 200 μL media or 2 days incubation in 400 μL media). However, the optimal period was 1 day culture in 200 μL media because the likelihood of microbial contamination increases with culture time. This culture period extended from 24 h to 48 h after worms were harvested from mice, after which point control (DMSO treated) wells were visibly yellow due to acidification with accumulated lactate. Media was removed and stored in sealed plates at –80°C, until lactate was measured with the Lactate-Glo assay kit (Promega). The lactate assay provides an indirect readout of lactate levels in the sample and is provided as a lactate detection reagent consisting of recombinant lactate-dehydrogenase, NAD⁺, luciferase, and luciferin detection solution. When L-lactate is present in the sample, recombinant lactate dehydrogenase generates NADH, which reduces the inactive form of luciferin to an activated form resulting in luminescence. To perform the test within the dynamic range of the assay kit, all samples were first diluted 1:250 in PBS. 25 μL of this diluted sample was added to solid white half area 96-well plates, followed by addition of 25 μL lactate detection reagent using a multichannel pipette. Plates were read on a SpectraMax i3x Multi-Mode Microplate Reader (Molecular Devices) in luminescence mode.

Miracidia motility assays. Livers harvested from schistosome-infected mice were processed to retrieve eggs and hatch miracidia as described previously (77). Ten livers were processed at a time. Briefly, livers were washed in saline (1.2% NaCl) and homogenized using a stainless-steel blender for 1 min. The volume of the resulting homogenate was brought to approximately 800 mL with fresh saline and centrifuged at 290 × *g* for 15 min at 4°C. The pellet was resuspended in saline and the wash step repeated, and the resulting purified eggs were resuspended in artificial pond water (final salt concentrations of CaCO₃ 66.6 μM, MgCO₃ 7.9 μM, NaCl 11.4 μM, KCl 1.8 μM) in a 1-L volumetric flask covered with foil up to the neck and hatching was facilitated with

a light source directed toward the flask neck. Concentrated hatched miracidia were collected from the top layer of pond water, and the volume was brought to 24 mL with pond water. Miracidia were then aliquoted 0.5 mL per well in 24-well plates (approximately 300 miracidia per well) and treated with test compounds for 1 h. Videos (30 s) were recorded using a stereomicroscope (Zeiss Stemi 508 with AxioCam 208 camera), converted to avi format using FFmpeg and processed in ImageJ.

In vivo drug screening. At 6 weeks postinfection, *S. mansoni*-infected mice were administered a single dose of test compound (ivermectin 10 mg/kg, doramectin 30 mg/kg, 23-ketonadectin 12.5 mg/kg, milbemyacin oxime 100 mg/kg, emamectin 20 mg/kg, eprinomectin 20 mg/kg, meclonazepam 30 mg/kg) solubilized in vegetable oil (0.25 mL) and delivered by oral gavage. These doses were selected based on the toxicity of each compound. Mice were euthanized as outlined above (CO₂ asphyxiation followed by cervical dislocation) at 7 weeks postinfection and worms were dissected from the liver and mesenteries to determine parasite burden for each mouse.

SUPPLEMENTAL MATERIAL

Supplemental material is available online only.

SUPPLEMENTAL FILE 1, PDF file, 1.7 MB.

SUPPLEMENTAL FILE 2, XLSX file, 0.2 MB.

ACKNOWLEDGMENTS

Schistosome infected mice were provided by the NIH-NIAID Schistosomiasis Resource Center for distribution through BEI Resources, NIH-NIAID Contract HHSN272201700014I. This work was supported by funding from NIH-NIAID R21AI146540 (J.D.C.), R21AI153545 (J.D.C. & M.Z.) and 5T32GM081061-04 (K.T.R.).

REFERENCES

- Nixon SA, Welz C, Woods DJ, Costa-Junior L, Zamanian M, Martin RJ. 2020. Where are all the anthelmintics? Challenges and opportunities on the path to new anthelmintics. *Int J Parasitol Drugs Drug Resist* 14:8–16. <https://doi.org/10.1016/j.ijpddr.2020.07.001>.
- Ismail M, Metwally A, Farghaly A, Bruce J, Tao LF, Bennett JL. 1996. Characterization of isolates of *Schistosoma mansoni* from Egyptian villagers that tolerate high doses of praziquantel. *Am J Trop Med Hyg* 55:214–218. <https://doi.org/10.4269/ajtmh.1996.55.214>.
- Danso-Appiah A, De Vlas SJ. 2002. Interpreting low praziquantel cure rates of *Schistosoma mansoni* infections in Senegal. *Trends Parasitol* 18: 125–129. [https://doi.org/10.1016/s1471-4922\(01\)02209-7](https://doi.org/10.1016/s1471-4922(01)02209-7).
- Kron M, Gordon C, Bauers T, Lu Z, Mahatme S, Shah J, Saeian K, McManus DP. 2019. Persistence of *Schistosoma japonicum* DNA in a kidney-liver transplant recipient. *Am J Trop Med Hyg* 100:584–587. <https://doi.org/10.4269/ajtmh.18-0752>.
- Fallon PG, Doenhoff MJ. 1994. Drug-resistant schistosomiasis: resistance to praziquantel and oxamniquine induced in *Schistosoma mansoni* in mice is drug specific. *Am J Trop Med Hyg* 51:83–88. <https://doi.org/10.4269/ajtmh.1994.51.83>.
- Le Clec'h W, Chevalier FD, Mattos ACA, Strickland A, Diaz R, McDew-White M, Rohr CM, Kinung'hi S, Allan F, Webster BL, Webster JP, Emery AM, Rollinson D, Djirmay AG, Al Mashikhi KM, Al Yafae S, Idris MA, Moné H, Mouahid G, LoVerde P, Marchant JS, Anderson TJ. 2021. Genetic analysis of praziquantel response in schistosome parasites implicates a transient receptor potential channel. *Sci Transl Med* 13:eabj9114. <https://doi.org/10.1126/scitranslmed.abj9114>.
- Chen S, Suzuki BM, Dohrmann J, Singh R, Arkin MR, Caffrey CR. 2020. A multi-dimensional, time-lapse, high content screening platform applied to schistosomiasis drug discovery. *Commun Biol* 3:747. <https://doi.org/10.1038/s42003-020-01402-5>.
- Diaz Soria CL, Lee J, Chong T, Coghlan A, Tracey A, Young MD, Andrews T, Hall C, Ng BL, Rawlinson K, Doyle SR, Leonard S, Lu Z, Bennett HM, Rinaldi G, Newmark PA, Berriman M. 2020. Single-cell atlas of the first intra-mammalian developmental stage of the human parasite *Schistosoma mansoni*. *Nat Commun* 11:6411. <https://doi.org/10.1038/s41467-020-20092-5>.
- Wendt G, Zhao L, Chen R, Liu C, O'Donoghue AJ, Caffrey CR, Reese ML, Collins JJ, 3rd. 2020. A single-cell RNA-seq atlas of *Schistosoma mansoni* identifies a key regulator of blood feeding. *Science* 369:1644–1649. <https://doi.org/10.1126/science.abb7709>.
- Wangwiwatsin A, Protasio AV, Wilson S, Owusu C, Holroyd NE, Sanders MJ, Keane J, Doenhoff MJ, Rinaldi G, Berriman M. 2020. Transcriptome of the parasitic flatworm *Schistosoma mansoni* during intra-mammalian development. *PLoS Negl Trop Dis* 14:e0007743. <https://doi.org/10.1371/journal.pntd.0007743>.
- Reimers N, Homann A, Hoschler B, Langhans K, Wilson RA, Pierrot C, Khalife J, Grevelding CG, Chalmers IW, Yazdanbakhsh M, Hoffmann KF, Hokke CH, Haas H, Schramm G. 2015. Drug-induced exposure of *Schistosoma mansoni* antigens SmCD59a and SmKK7. *PLoS Negl Trop Dis* 9:e0003593. <https://doi.org/10.1371/journal.pntd.0003593>.
- Martin RJ, Robertson AP, Choudhary S. 2021. Ivermectin: an anthelmintic, an insecticide, and much more. *Trends Parasitol* 37:48–64. <https://doi.org/10.1016/j.pt.2020.10.005>.
- Sigel E, Baur R. 1987. Effect of avermectin B1a on chick neuronal gamma-aminobutyrate receptor channels expressed in *Xenopus* oocytes. *Mol Pharmacol* 32:749–752.
- Krause RM, Buisson B, Bertrand S, Corringier P-J, Galzi J-L, Changeux J-P, Bertrand D. 1998. Ivermectin: a positive allosteric effector of the $\alpha 7$ neuronal nicotinic acetylcholine receptor. *Mol Pharmacol* 53:283–294. <https://doi.org/10.1124/mol.53.2.283>.
- Khakh BS, Proctor WR, Dunwiddie TV, Labarca C, Lester HA. 1999. Allosteric control of gating and kinetics at P2X4 receptor channels. *J Neurosci* 19:7289–7299. <https://doi.org/10.1523/JNEUROSCI.19-17-07289.1999>.
- Shan Q, Haddrill JL, Lynch JW. 2001. Ivermectin, an unconventional agonist of the glycine receptor chloride channel. *J Biol Chem* 276:12556–12564. <https://doi.org/10.1074/jbc.M011264200>.
- Campbell WC, Fisher MH, Stapley EO, Albers-Schönberg G, Jacob TA. 1983. Ivermectin: a potent new antiparasitic agent. *Science* 221:823–828. <https://doi.org/10.1126/science.6308762>.
- Campbell WC. 1991. Ivermectin as an antiparasitic agent for use in humans. *Annu Rev Microbiol* 45:445–474. <https://doi.org/10.1146/annurev.mi.45.100191.002305>.
- Shoop WL, Ostlind DA, Rohrer SP, Mickle G, Haines HW, Michael BF, Mrozik H, Fisher MH. 1995. Avermectins and milbemycins against *Fasciola hepatica*: in vivo drug efficacy and in vitro receptor binding. *Int J Parasitol* 25:923–927. [https://doi.org/10.1016/0020-7519\(95\)00026-x](https://doi.org/10.1016/0020-7519(95)00026-x).
- Vicente B, López-Abán J, Chaccour J, Hernández-Goenaga J, Nicolas P, Fernández-Soto P, Muro A, Chaccour C. 2021. The effect of ivermectin alone and in combination with cobicistat or elacridar in experimental *Schistosoma mansoni* infection in mice. *Sci Rep* 11:4476. <https://doi.org/10.1038/s41598-021-84009-y>.
- Dufour V, Beech RN, Wever C, Dent JA, Geary TG. 2013. Molecular cloning and characterization of novel glutamate-gated chloride channel subunits from *Schistosoma mansoni*. *PLoS Pathog* 9:e1003586. <https://doi.org/10.1371/journal.ppat.1003586>.
- Katz N, Araújo N, Coelho PMZ, Morel CM, Linde-Arias AR, Yamada T, Horimatsu Y, Suzuki K, Sunazuka T, Omura S. 2017. Ivermectin efficacy against *Biomphalaria*, intermediate host snail vectors of *Schistosomiasis*. *J Antibiot (Tokyo)* 70:680–684. <https://doi.org/10.1038/ja.2017.31>.
- Nogi T, Zhang D, Chan JD, Marchant JS. 2009. A novel biological activity of praziquantel requiring voltage-operated Ca²⁺ channel β subunits: subversion of flatworm regenerative polarity. *PLoS Negl Trop Dis* 3:e464. <https://doi.org/10.1371/journal.pntd.0000464>.

24. Simanov D, Mellaart-Straver I, Sormacheva I, Berezikov E. 2012. The flatworm *Macrostomum lignano* is a powerful model organism for ion channel and stem cell research. *Stem Cells Int* 2012:167265. <https://doi.org/10.1155/2012/167265>.
25. Ferenc NN, Levin M. 2019. Effects of ivermectin exposure on regeneration of *D. dorotocephala planaria*: exploiting human-approved ion channel drugs as morphochemicals. *Macromol Biosci* 19:e1800237. <https://doi.org/10.1002/mabi.201800237>.
26. Shoop WL, Mrozik H, Fisher MH. 1995. Structure and activity of avermectins and milbemycins in animal health. *Vet Parasitol* 59:139–156. [https://doi.org/10.1016/0304-4017\(94\)00743-v](https://doi.org/10.1016/0304-4017(94)00743-v).
27. Barda B, Coulibaly JT, Puchkov M, Huwyler J, Hattendorf J, Keiser J. 2016. Efficacy and safety of moxidectin, synriam, synriam-praziquantel versus praziquantel against schistosoma haematobium and *S. mansoni* infections: a randomized, exploratory phase 2 trial. *PLoS Negl Trop Dis* 10:e0005008. <https://doi.org/10.1371/journal.pntd.0005008>.
28. Panic G, Vargas M, Scandale I, Keiser J. 2015. Activity profile of an FDA-approved compound library against *Schistosoma mansoni*. *PLoS Negl Trop Dis* 9:e0003962. <https://doi.org/10.1371/journal.pntd.0003962>.
29. Zorn KM, Sun S, McConnon CL, Ma K, Chen EK, Foil DH, Lane TR, Liu LJ, El-Sakkary N, Skinner DE, Ekins S, Caffrey CR. 2021. A machine learning strategy for drug discovery identifies anti-schistosomal small molecules. *ACS Infect Dis* 7:406–420. <https://doi.org/10.1021/acinfeddis.0c00754>.
30. Ramirez B, Bickle Q, Yousif F, Fakorede F, Mouries MA, Nwaka S. 2007. Schistosomes: challenges in compound screening. *Expert Opin Drug Discov* 2:553–61. <https://doi.org/10.1517/17460441.2.S1.553>.
31. Marcellino C, Gut J, Lim KC, Singh R, McKerrow J, Sakanari J. 2012. Worm-Assay: a novel computer application for whole-plate motion-based screening of macroscopic parasites. *PLoS Negl Trop Dis* 6:e1494. <https://doi.org/10.1371/journal.pntd.0001494>.
32. Wheeler NJ, Heimark ZW, Airs PM, Mann A, Bartholomay LC, Zamanian M. 2020. Genetic and functional diversification of chemosensory pathway receptors in mosquito-borne filarial nematodes. *PLoS Biol* 18:e3000723. <https://doi.org/10.1371/journal.pbio.3000723>.
33. Wheeler NJ, Gallo KJ, Rehborg EJG, Ryan KT, Chan JD, Zamanian M. 2022. wormXpress: a modular package for high-throughput image analysis of parasitic and free-living worms. *PLoS Negl Trop Dis* 16:e010937. <https://doi.org/10.1371/journal.pntd.010937>.
34. Howe S, Zophel D, Subbaraman H, Unger C, Held J, Engleitner T, Hoffmann WH, Kreidenweiss A. 2015. Lactate as a novel quantitative measure of viability in *Schistosoma mansoni* drug sensitivity assays. *Antimicrob Agents Chemother* 59:1193–1199. <https://doi.org/10.1128/AAC.03809-14>.
35. Stohler HR. 1978. Ro 11–3128, a novel schistosomicidal compound. *Current chemotherapy* 1:147–148.
36. Barker LR, Bueding E, Timms AR. 1966. The possible role of acetylcholine in *Schistosoma mansoni*. *Br J Pharmacol Chemother* 26:656–665. <https://doi.org/10.1111/j.1476-5381.1966.tb01845.x>.
37. Mellin TN, Busch RD, Wang CC, Kath G. 1983. Neuropharmacology of the parasitic trematode, *Schistosoma mansoni*. *Am J Trop Med Hyg* 32:83–93. <https://doi.org/10.4269/ajtmh.1983.32.83>.
38. Chan JD, Day TA, Marchant JS. 2018. Coalescing beneficial host and deleterious antiparasitic actions as an antischistosomal strategy. *Elife* 7. <https://doi.org/10.7554/eLife.35755>.
39. Bueding E. 1950. Carbohydrate metabolism of schistosoma mansoni. *J Gen Physiol* 33:475–495. <https://doi.org/10.1085/jgp.33.5.475>.
40. Bueding E, Fisher J. 1982. Metabolic requirements of schistosomes. *J Parasitol* 68:208–212. <https://doi.org/10.2307/3281177>.
41. Wolstenholme AJ, Neveu C. 2022. The avermectin/milbemycin receptors of parasitic nematodes. *Pestic Biochem Physiol* 181:105010. <https://doi.org/10.1016/j.pestbp.2021.105010>.
42. McCusker P, Mian MY, Li G, Olp MD, Tiruveedhula V, Rashid F, Golani LK, Verma RS, Smith BC, Cook JM, Chan JD. 2019. Non-sedating benzodiazepines cause paralysis and tissue damage in the parasitic blood fluke *Schistosoma mansoni*. *PLoS Negl Trop Dis* 13:e0007826. <https://doi.org/10.1371/journal.pntd.0007826>.
43. Andrews P. 1978. Effect of praziquantel on the free living stages of *Schistosoma mansoni*. *Z Parasitenkd* 56:99–106. <https://doi.org/10.1007/BF00925943>.
44. Baard AP, Sommers DK, Honiball PJ, Fourie ED, Du Toit LE. 1979. Preliminary results in human schistosomiasis with Ro 11–3128. *S Afr Med J* 55:617–618.
45. Merck Research Laboratories. 1996. FDA approval package application # 050742.
46. Committee for Veterinary Medicinal Products. 1999. European Agency for the Evaluation of Medicinal Products Summary Report on Emamectin.
47. Xu Q, Li J, Qu M, Zhang Y, Yu X, Xiang W. 2010. Acute toxicity of milbemycin oxime in mice. 4th International Conference on Bioinformatics and Biomedical Engineering. <https://doi.org/10.1109/icbbe.2010.55116689>.
48. Wählby C, Kamensky L, Liu ZH, Riklin-Raviv T, Conery AL, O'Rourke EJ, Sokolnicki KL, Visvikis O, Ljosa V, Irazoqui JE, Golland P, Ruvkun G, Ausubel FM, Carpenter AE. 2012. An image analysis toolbox for high-throughput *C. elegans* assays. *Nat Methods* 9:714–716. <https://doi.org/10.1038/nmeth.1984>.
49. McDermott-Rouse A, Minga E, Barlow I, Feriani L. 2021. Behavioral fingerprints predict insecticide and anthelmintic mode of action. *bioRxiv*.
50. Zamanian M, Chan JD. 2021. High-content approaches to anthelmintic drug screening. *Trends Parasitol* 37:780–789. <https://doi.org/10.1016/j.pt.2021.05.004>.
51. Wheeler NJ, Ryan KT, Gallo KJ, Henthorn CR, Ericksen SS, Chan JD, Zamanian M. 2022. Multivariate chemogenomic screening prioritizes new macrofilaricidal leads. *bioRxiv*.
52. Barlow IL, Feriani L, Minga E, McDermott-Rouse A, O'Brien TJ, Liu Z, Hofbauer M, Stowers JR, Ding SS, Brown AEX. 2022. Megapixel camera arrays enable high-resolution animal tracking in multiwell plates. *Comm Bio* 5:253. <https://doi.org/10.1038/s42003-022-03206-1>.
53. Maccesi M, Aguiar PHN, Pasche V, Padilla M, Suzuki BM, Montefusco S, Abagyan R, Keiser J, Mourão MM, Caffrey CR. 2019. Multi-center screening of the Pathogen Box collection for schistosomiasis drug discovery. *Parasit Vectors* 12:493. <https://doi.org/10.1186/s13071-019-3747-6>.
54. Peña-Silva R, Duffull SB, Steer AC, Jaramillo-Rincon SX, Gwee A, Zhu X. 2021. Pharmacokinetic considerations on the repurposing of ivermectin for treatment of COVID-19. *Br J Clin Pharmacol* 87:1589–1590. <https://doi.org/10.1111/bcp.14476>.
55. Michael B, Meinke PT, Shoop W. 2001. Comparison of ivermectin, doramectin, selamectin, and eleven intermediates in a nematode larval development assay. *J Parasitol* 87:692–696. [https://doi.org/10.1645/0022-3395\(2001\)087\[0692:COIDSA\]2.0.CO;2](https://doi.org/10.1645/0022-3395(2001)087[0692:COIDSA]2.0.CO;2).
56. Dent JA, Smith MM, Vassilatis DK, Avery L. 2000. The genetics of ivermectin resistance in *Caenorhabditis elegans*. *Proc Natl Acad Sci U S A* 97:2674–2679. <https://doi.org/10.1073/pnas.97.6.2674>.
57. Moreno Y, Nabhan JF, Solomon J, Mackenzie CD, Geary TG. 2010. Ivermectin disrupts the function of the excretory-secretory apparatus in microfilariae of *Brugia malayi*. *Proc Natl Acad Sci U S A* 107:20120–20125. <https://doi.org/10.1073/pnas.1011983107>.
58. Harischandra H, Yuan W, Loghry HJ, Zamanian M, Kimber MJ. 2018. Profiling extracellular vesicle release by the filarial nematode *Brugia malayi* reveals sex-specific differences in cargo and a sensitivity to ivermectin. *PLoS Negl Trop Dis* 12:e0006438. <https://doi.org/10.1371/journal.pntd.0006438>.
59. Loghry HJ, Yuan W, Zamanian M, Wheeler NJ, Day TA, Kimber MJ. 2020. Ivermectin inhibits extracellular vesicle secretion from parasitic nematodes. *J Extracell Vesicles* 10:e12036. <https://doi.org/10.1002/jev.2.12036>.
60. Henthorn CR, Airs PM, Neumann E, Zamanian M. 2022. Resolving the origins of secretory products and anthelmintic responses in a human parasitic nematode at single-cell resolution. *bioRxiv*.
61. Laing R, Gillan V, Devaney E. 2017. Ivermectin - old drug, new tricks? *Trends Parasitol* 33:463–472. <https://doi.org/10.1016/j.pt.2017.02.004>.
62. Chen I-S, Kubo Y. 2018. Ivermectin and its target molecules: shared and unique modulation mechanisms of ion channels and receptors by ivermectin. *J Physiol* 596:1833–1845. <https://doi.org/10.1113/JP275236>.
63. Lynch T, Lynch JW. 2010. A glycine residue essential for high ivermectin sensitivity in Cys-loop ion channel receptors. *Int J Parasitol* 40:1477–1481. <https://doi.org/10.1016/j.ijpara.2010.07.010>.
64. Lynch T, Lynch JW. 2012. Ivermectin binding sites in human and invertebrate Cys-loop receptors. *Trends Pharmacol Sci* 33:432–441. <https://doi.org/10.1016/j.tips.2012.05.002>.
65. Collins T, Millar NS. 2010. Nicotinic acetylcholine receptor transmembrane mutations convert ivermectin from a positive to a negative allosteric modulator. *Mol Pharmacol* 78:198–204. <https://doi.org/10.1124/mol.110.064295>.
66. Zheng Y, Hirschberg B, Yuan J, Wang AP, Hunt DC, Ludmerer SW, Schmatz DM, Cully DF. 2002. Identification of two novel *Drosophila melanogaster* histamine-gated chloride channel subunits expressed in the eye. *J Biol Chem* 277:2000–2005. <https://doi.org/10.1074/jbc.M107635200>.
67. MacDonald K, Buxton S, Kimber MJ, Day TA, Robertson AP, Ribeiro P. 2014. Functional characterization of a novel family of acetylcholine-gated chloride channels in *Schistosoma mansoni*. *PLoS Pathog* 10:e1004181. <https://doi.org/10.1371/journal.ppat.1004181>.
68. Bentley GN, Jones AK, Oliveros Parra WG, Agnew A. 2004. ShAR1 α and ShAR1 β : novel putative nicotinic acetylcholine receptor subunits from the platyhelminth blood fluke *Schistosoma*. *Gene* 329:27–38. <https://doi.org/10.1016/j.gene.2003.12.009>.

69. Jaiteh M, Taly A, Hénin J. 2016. Evolution of pentameric ligand-gated ion channels: pro-loop receptors. *PLoS One* 11:e0151934. <https://doi.org/10.1371/journal.pone.0151934>.
70. Perry T, McKenzie JA, Batterham P. 2007. A D α 6 knockout strain of *Drosophila melanogaster* confers a high level of resistance to spinosad. *Insect Biochem Mol Biol* 37:184–188. <https://doi.org/10.1016/j.ibmb.2006.11.009>.
71. Puinean AM, Lansdell SJ, Collins T, Bielza P, Millar NS. 2013. A nicotinic acetylcholine receptor transmembrane point mutation (G275E) associated with resistance to spinosad in *Frankliniella occidentalis*. *J Neurochem* 124: 590–601. <https://doi.org/10.1111/jnc.12029>.
72. Somers J, Nguyen J, Lumb C, Batterham P, Perry T. 2015. In vivo functional analysis of the *Drosophila melanogaster* nicotinic acetylcholine receptor D α 6 using the insecticide spinosad. *Insect Biochem Mol Biol* 64:116–127. <https://doi.org/10.1016/j.ibmb.2015.01.018>.
73. Zimmer CT, Garrod WT, Puinean AM, Eckel-Zimmer M, Williamson MS, Davies TGE, Bass C. 2016. A CRISPR/Cas9 mediated point mutation in the alpha 6 subunit of the nicotinic acetylcholine receptor confers resistance to spinosad in *Drosophila melanogaster*. *Insect Biochem Mol Biol* 73: 62–69. <https://doi.org/10.1016/j.ibmb.2016.04.007>.
74. Lu W, Liu Z, Fan X, Zhang X, Qiao X, Huang J. 2022. Nicotinic acetylcholine receptor modulator insecticides act on diverse receptor subtypes with distinct subunit compositions. *PLoS Genet* 18:e1009920. <https://doi.org/10.1371/journal.pgen.1009920>.
75. Xu X, Sepich C, Lukas RJ, Zhu G, Chang Y. 2016. Emamectin is a non-selective allosteric activator of nicotinic acetylcholine receptors and GABA A /C receptors. *Biochem Biophys Res Commun* 473:795–800. <https://doi.org/10.1016/j.bbrc.2016.03.097>.
76. Noonan JD, Beech RN. 2022. Reconstitution of an N-AChR from *Brugia malayi*. *bioRxiv*.
77. Dinguirard N, Heinemann C, Yoshino TP. 2018. Mass isolation and *in vitro* cultivation of intramolluscan stages of the human blood fluke *Schistosoma mansoni*. *J Vis Exp* 14:56345. <https://doi.org/10.3791/56345>.